Cuvier's beaked whale (*Ziphius cavirostris*) head tissues: physical properties and CT imaging

Melissa S. Soldevilla[1,*], Megan F. McKenna[2], Sean M. Wiggins[1], Robert E. Shadwick[1], Ted W. Cranford[2] and John A. Hildebrand[1]

[1]*Scripps Institution of Oceanography, University of California, San Diego, 9500 Gilman Drive, La Jolla, CA 92093-0205, USA* and [2]*San Diego State University, 5500 Campanile Drive, San Diego, CA 92182, USA*

*Author for correspondence (e-mail: mhock@ucsd.edu)

Summary

Tissue physical properties from a Cuvier's beaked whale (*Ziphius cavirostris*) neonate head are reported and compared with computed tomography (CT) X-ray imaging. Physical properties measured include longitudinal sound velocity, density, elastic modulus and hysteresis. Tissues were classified by type as follows: mandibular acoustic fat, mandibular blubber, forehead acoustic fat (melon), forehead blubber, muscle and connective tissue. Results show that each class of tissues has unique, co-varying physical properties. The mandibular acoustic fats had minimal values for sound speed (1350 ± 10.6 m s^{-1}) and mass density (890 ± 23 kg m^{-3}). These values increased through mandibular blubber (1376 ± 13 m s^{-1}, 919 ± 13 kg m^{-3}), melon (1382 ± 23 m s^{-1}, 937 ± 17 kg m^{-3}), forehead blubber (1401 ± 7.8 m s^{-1}, 935 ± 25 kg m^{-3}) and muscle (1517 ± 46.8 m s^{-1}, 993 ± 58 kg m^{-3}). Connective tissue had the greatest mean sound speed and density (1628 ± 48.7 m s^{-1}, 1087 ± 41 kg m^{-3}). The melon formed a low-density, low-sound-speed core, supporting its function as a sound focusing organ. Hounsfield unit (HU) values from CT X-ray imaging are correlated with density and sound speed values, allowing HU values to be used to predict these physical properties. Blubber and connective tissues have a higher elastic modulus than acoustic fats and melon, suggesting more collagen structure in blubber and connective tissues. Blubber tissue elastic modulus is nonlinear with varying stress, becoming more incompressible as stress is increased. These data provide important physical properties required to construct models of the sound generation and reception mechanisms in *Ziphius cavirostris* heads, as well as models of their interaction with anthropogenic sound.

Key words: Cuvier's beaked whale, *Ziphius cavirostris*, physical property, sound speed, density, Hounsfield unit, elastic modulus.

Introduction

Cuvier's beaked whale (*Ziphius cavirostris*) is the most abundant species of the Ziphiidae family of toothed whales (Heyning, 1989b), yet much about it remains unknown. Studies of live *Z. cavirostris* are rare, as they are visually inconspicuous at sea due to deep, long-duration dives and short surface times (Heyning, 1989b; Barlow et al., 1997; Baird et al., 2004). Cuvier's beaked whales typically inhabit deep, offshore waters exhibiting steep slope features such as submarine canyons, oceanic islands, the continental shelf edge, and enclosed seas (Boutiba, 1994; D'Amico et al., 2003; Forney et al., 1995; Heyning, 1989b; Houston, 1991; Marini et al., 1996; Waring et al., 2001). Similar to other toothed whales, echolocation is important for Cuvier's beaked whales when navigating these features and when foraging for deep-sea and benthic squid, fish and crustaceans in the mesopelagic zone (Blanco and Raga, 2000; Fiscus, 1997; Johnson et al., 2004; MacLeod et al., 2003; Santos et al., 2001). Recently, the use of high-intensity anthropogenic sounds, particularly mid-frequency (2–4 kHz) sonar, has been associated with mass strandings of Cuvier's beaked whales (Evans and England, 2001; Frantzis, 1998; Simmonds and Lopez-Jurado, 1991). Physiological mechanisms including rectified diffusion of gas bubbles in tissues (Crum and Mao, 1996; Houser et al., 2001), gas emboli formation in body fats (Jepson et al., 2003; Fernandez et al., 2004) or bubble or lung resonance (Finneran, 2003) may explain the observed hemorrhaging in the lungs, acoustic pathways, brain, spinal cord, kidneys and eyes, congestion and bubbles in the brain, and embolisms in body fats in stranded animals (Evans and England, 2001; Fernandez et al., 2004). The role that sound exposure played in these strandings and subsequent deaths remains controversial. Models of sound propagation within these beaked whales may provide insight into questions about their response to sound exposure, echolocation production and sound reception.

Sound production systems in beaked whales may be similar to those found in other odontocetes. Comparative anatomic

studies highlight homologous structures responsible for sound generation associated with echolocation, which are unique among mammals (Au, 1993; Cranford et al., 1996; Heyning, 1989a; Heyning and Mead, 1990; Lawrence and Schevill, 1956; Mead, 1975). Convincing evidence suggests that echolocation clicks are produced at the phonic lips [a structural complex previously known as the monkey lips/dorsal bursae (MLDB) region; Cranford et al., 1996; Aroyan et al., 1992] and then progressively focused by the skull, air spaces, connective tissue sheaths and gradients within the melon, before propagating into the external environment. The melon, a complex connective tissue and lipid structure located in the forehead region of all odontocetes (Cranford et al., 1996), is likely to be important in the sound production system of *Z. cavirostris* (Fig. 1).

Morphological studies of homology across odontocetes suggest that the sound reception system in beaked whales is similar to the system found in better-studied odontocete species (Au, 1993). The odontocete sound reception pathway involves transmission through bone and lipids of the lower jaw, rather than through the tympanic membrane, as is typical in terrestrial mammals. Sound waves are directed towards the inner ear complex through a system that includes fat bodies lining the interior and exterior mandibles, thin translucent regions of bones in the posterior portion of the lower jaws, and air sinuses (Aroyan, 2001; Brill et al., 1988; Figs 1, 2). Norris (1968) coined the term 'acoustic fats' to describe these mandibular fat bodies, as well as the fats in the melon, due to their proposed role in sound propagation. The air spaces are excellent acoustic reflectors that may function to shield the ear complex from internally produced sounds and isolate them acoustically to facilitate directional hearing (Norris, 1964).

Sound propagation modeling has been used only recently to investigate sound pathways in marine mammals. Aroyan et al. (1992) and Aroyan (2001) explored sound emission and reception in a common dolphin, *Delphinus delphis*, by combining three-dimensional acoustic propagation models with topographical X-ray computed tomography (CT) data. While these models show great promise for understanding sound propagation in marine mammals, they only used simplified estimates and assumptions of tissue properties, such as sound speed and density, and they do not consider the elastic properties of the tissues (Aroyan et al., 1992; Aroyan,
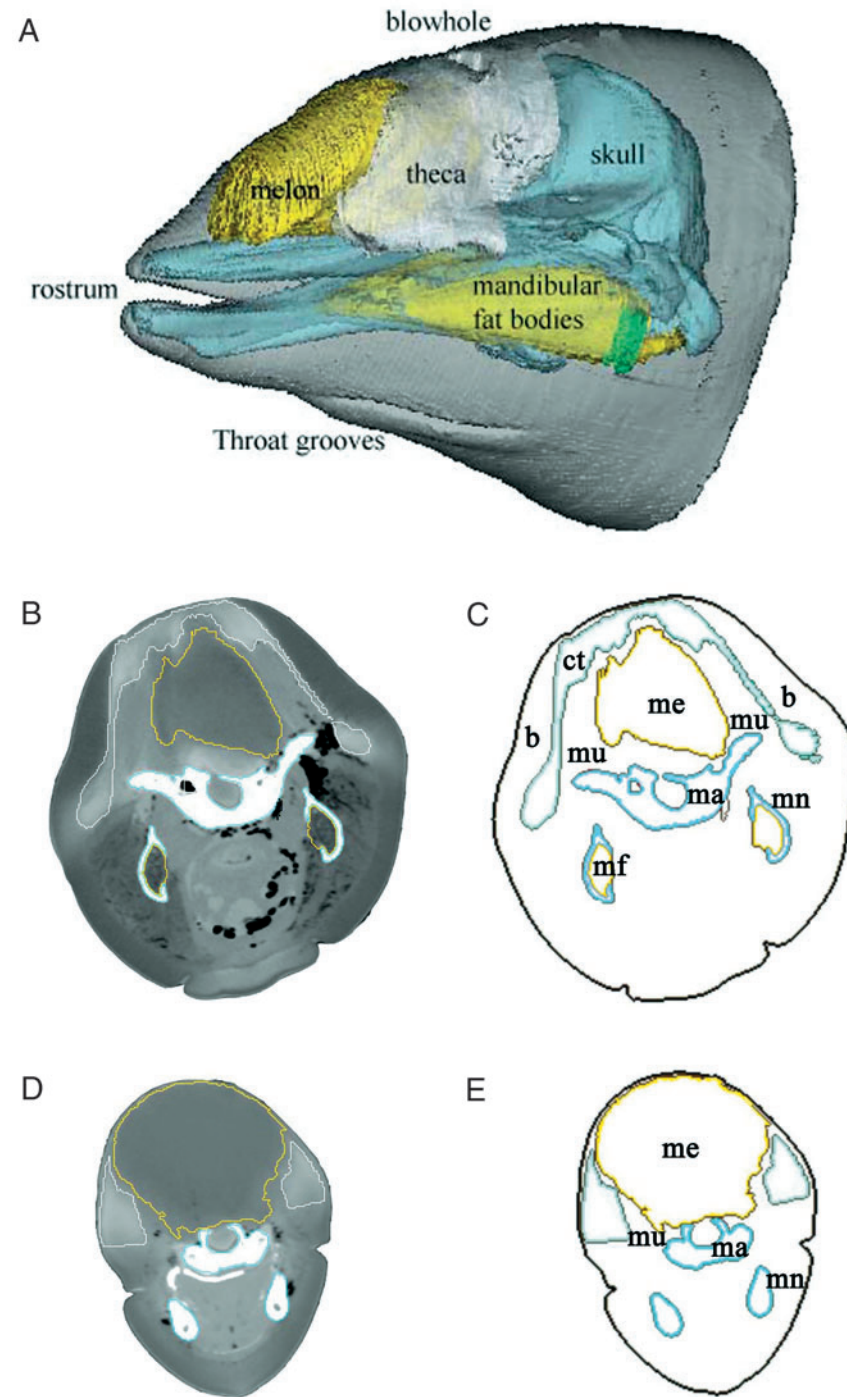

Fig. 1. (A) Reconstructed computer image of a neonate *Z. cavirostris* head. Dark grey areas show the outer skin layer. The light blue region is bone, i.e. the skull and mandible. The white area is the connective tissue theca that encompasses the melon, seen in yellow. Mandibular fat bodies are also shown in yellow. Colorized CT scans of transverse slices through (B) a posterior region and (D) an anterior region of the head. C and E represent line drawings that diagram the body parts seen in scans B and D, respectively. Abbreviations: b, blubber; ct, connective tissue; ma, maxilla; me, melon; mf, mandibular fat; mn, mandibular bones; mu, muscle. Only interior mandibular fat is represented in these images.
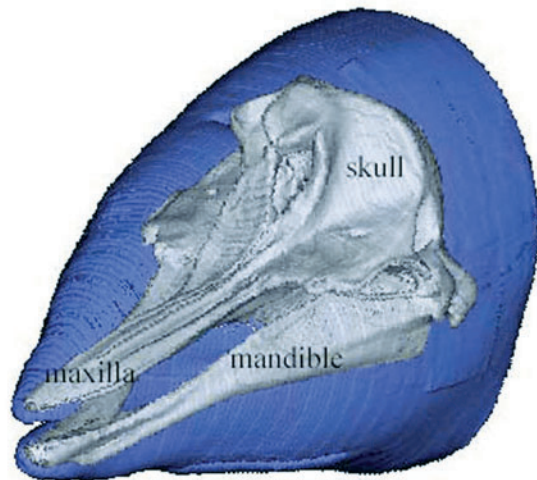
Fig. 2. *Ziphius cavirostris* skull. The concave skull basin where the melon is located is readily apparent. The hollowed mandibles, which house the acoustic fats important to sound reception, are also noted.

Table 1. *List of samples used in the physical properties analysis of a* Ziphius cavirostris *neonate head*

Sample name	Tissue category	Slice name	Samples/ slice
Left mandible acoustic blubber	Blubber	A–J	1
Left mandible external acoustic fat	Acoustic fat	A–L	1
Left mandible internal acoustic fat	Acoustic fat	A	1
Left mandible internal acoustic fat	Acoustic fat	B	2
Left mandible internal acoustic fat	Acoustic fat	C	2
Left mandible internal acoustic fat	Acoustic fat	D	2
Left mandible internal acoustic fat	Acoustic fat	E	4
Left mandible internal acoustic fat	Acoustic fat	F	5
Left mandible internal acoustic fat	Acoustic fat	G	5
Left mandible internal acoustic fat	Acoustic fat	H	6
Left mandible internal acoustic fat	Acoustic fat	I	6
Left mandible internal acoustic fat	Acoustic fat	J	5
Left mandible internal acoustic fat	Acoustic fat	K	7
Forehead	Variable	A	3
Forehead	Variable	B	6
Forehead	Variable	C	9
Forehead	Variable	D	11
Forehead	Variable	E	13
Forehead	Variable	F	17
Forehead	Variable	G	17
Forehead	Variable	H	20
Forehead	Variable	I	23
Forehead	Variable	J	16
Forehead	Variable	K	31
Forehead	Variable	L	20
Forehead	Variable	M	14
Forehead	Variable	N/O	3

2001). The inclusion of measured tissue properties in sound propagation models will provide a more accurate representation of the complexities of sound emission and reception in these marine mammals.

Odontocete melon and mandibular fat bodies exhibit structural and chemical complexity that could have important implications for sound emission and reception. Structurally, the melon is comprised of gradations of tissues, with a central core of acoustic lipids grading into complex musculature, dense connective tissue (theca) and blubber, with notable topographical asymmetry (Heyning, 1989a; Cranford et al., 1996; Fig. 1). Studies of the chemical composition of melon acoustic lipids and mandibular fat bodies suggest complex chemical topography associated with acoustic functionality (Blomberg and Lindholm, 1976; Koopman et al., 2003; Litchfield et al., 1973; Varanasi et al., 1982). Sound speed in melon lipids has been shown to vary with chemical composition and topography in the melon (Blomberg and Jensen, 1976; Blomberg and Lindhom, 1976; Flewellen and Morris, 1978; Goold et al., 1996; Goold and Clarke, 2000; Litchfield et al., 1973, 1979; Norris and Harvey, 1974; Varanasi et al., 1982). Sound speed in the tissues surrounding the melon has not been studied. Understanding structural and compositional heterogeneity, and the resulting tissue physical properties, is invaluable for developing a good representative model of the acoustic pathways in the head of an odontocete whale.

To build representative acoustic-structural models of a Cuvier's beaked whale, high-resolution sound speed, density and elasticity measurements are needed; however, no data exist in the literature for this species. Fortunately, in 2002, we obtained a freshly stranded neonate Cuvier's beaked whale specimen for study. From the head of this specimen, we present approximately 200 measurements for tissue sound speed, density, CT scan Hounsfield unit (HU) values and elastic modulus that provide a basis for which to build an acoustic-structural model. We show that our methods provide comparable results to those from aquatic and terrestrial mammals. We show that sound speed values and topographical variations in a neonate Cuvier's beaked whale melon are similar to those in more-studied odontocete species. Finally, we provide a predictable relationship between the Hounsfield units from CT scans and measured tissue sound speed and density values.

Materials and methods

For CT imaging, dissection and tissue measurements, we obtained a carcass of a Cuvier's beaked whale, *Ziphius cavirostris* Cuvier (NMFS field number KXD0019). The 314.9 cm-long female neonate carcass, found on 7 January 2002 at Camp Pendleton in San Diego, CA, USA was determined by NMFS personnel to be freshly dead, with little evidence of decomposition. The animal was estimated to be about one month old at the time of death. Immediately after the body was recovered from the beach, it was completely frozen to −20°C. In April 2002, the frozen specimen was cut across the long axis of the body into four manageable segments using an industrial dual column band saw. The segments corresponded roughly to the head, thorax, abdomen and tail.
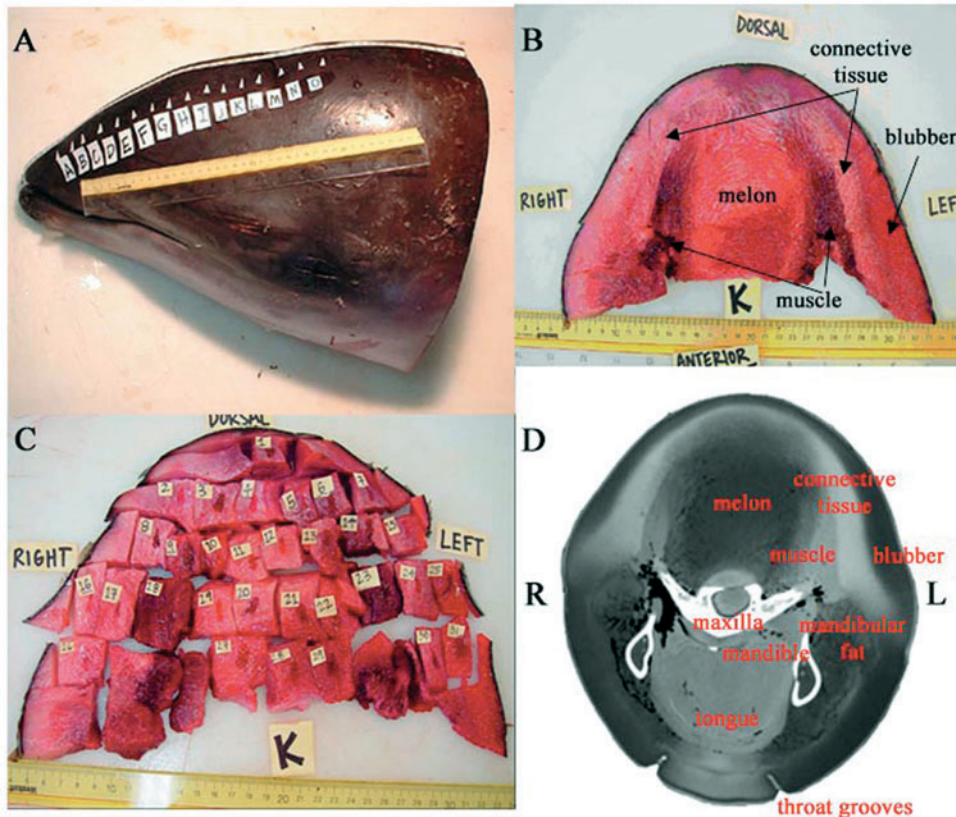
Fig. 3. (A) Head of a neonate *Z. cavirostris*. Arrowheads point to transverse slices (A–O) that were taken through the melon. (B) Anterior side of a transverse slice through the melon, which corresponds to slice K, from A. Skin, blubber, connective tissue, muscle and melon tissues are noted. (C) Transverse melon slice K, showing grid-like sampling of tissues into numbered cubes. (D) Transverse CT scan image of slice K. Maxillary and mandibular bones are visible as bright white areas. Between these is the tongue. A blubber sheath can be seen surrounding the animal. The connective tissue, muscle and melon fats can be discerned in the upper portion of the figure. Interior and exterior mandibular fats can be seen inside of and around the mandibular bones. Throat grooves are also visible.

The segments were individually thawed, CT scanned, dissected and cut into smaller pieces for further analysis. This report presents tissue properties for the head only; results from remaining segments and a more comprehensive list of measurement values for all segments can be found in Soldevilla et al. (2004).

CT scans

The head was thawed in a water bath for 48 h to ensure complete, consistent thawing and then subjected to CT scanning using a GE Light Speed Plus CT scanner. Axial scans, 5 mm thick, were collected every 5 mm, to ensure the entire specimen was scanned. The scanner used a 500 mm-diameter field of view scan region. Images were collected with a 140 kV×320 mA power setting. Image data were recorded directly to hard drive.

We analyzed the CT scan data after the dissection to determine HU values for the volumes representing the tissue samples used for physical property measurements. We used E-film, a specialized software package (Merge-efilm, Milwaukee, WI, USA), to convert CT units of electron density into calibrated HUs. HUs are scaled from –1000 to >1000, where air is at –1000, room temperature water is at 0, and hard bone can be found at >1000 (Robb, 1998). Mammalian soft tissues generally range between –100 and 100, with fatty tissues at the low end and denser connective tissues at the high end (Duck, 1990). HUs are standardized by defining water as zero and are calibrated such that one unit is equal to the change in the density of 1 cm^3 of water raised 1°C at standard temperature

and pressure. We referred to photos taken during the dissection to locate the position of dissected tissue samples in the CT scan images. We chose the CT image that corresponded to the center of each dissection slice by referring to landmarks such as the skull, eyes and ears. Samples were picked by visually correlating the CT image with the photo of each slice. HU values within a 50 mm^3 region were used to calculate a mean HU and standard deviation at the approximate center of each sample.

Dissection

A dissection was performed after the CT scan, with extra attention and finer scale sampling in the forehead and mandibular regions (see Table 1 for sample descriptions). The forehead was cut transversely into 2 cm-thick slices for a total of 15 slices (Fig. 3A,B). Each slice was further cut in a grid-like fashion into ~2 cm cubes (Fig. 3C) to provide high-resolution topographical data. The left mandibular region was also cut transversely into 2 cm-thick slices for a total of 12 slices. For each slice, one sample was taken from the blubber and the exterior mandibular fat, and 1–5 samples were taken from the interior mandibular fat. Each cubic sample was numbered, notched on the anterior right dorsal corner, and stained on the anterior side with Basic Fuchsin (Lillie, 1977) to provide sample location and orientation reference during post-dissection evaluation. The dissection was recorded photographically with a 5 megapixel digital color camera (Sony Cyber-shot DSC-707).

Tissue samples were visually categorized by color, texture

and location within the head into the following broad categories: blubber, acoustic fats (including melon and mandibular fat), muscle, and connective tissue. All samples containing a mixture of these categories were discarded from further analysis to provide homogeneous tissue samples for physical property measurements. Note that the tissue samples were categorized subjectively and, while more accurate descriptions of tissue could be determined by histological analysis, such an investigation was not within the scope of our analysis.

Sound velocity

Sound velocity was measured in each tissue sample using a Krautkramer Branson USD10 Ultrasonic Digital Flaw Detector and two Krautkramer Branson longitudinal acoustic transducers (Alpha series, 10 MHz, 0.25 mm; Krautkramer, General Electric Inspection Technologies, Hverth, Germany) attached to digital calipers (model no. CD-8″CS, Mitutoyo America Corp., Aurora, IL, USA). The Krautkramer velocimeter system measured the transmission time of 10 MHz broadband pulses through the various tissue samples. The calipers were used to measure the sample thickness to the nearest millimeter, and velocity was calculated by dividing the thickness by the travel time. Prior to measuring the samples, the velocimeter was calibrated using distilled water at room temperature (22.5°C), assuming a sound speed of 1490 m s^{-1} (Chen and Millero, 1977). Sound velocity was measured along three directions of each sample cube (anterior–posterior, dorsal–ventral, lateral) to test for anisotropy. Temperatures of the samples were recorded for later temperature–sound velocity normalization. Ultrasonic attenuation measurements were also made. Results of sound velocity anisotropy and ultrasonic attenuation are reported by Soldevilla et al. (2004). Sound velocity measurements were made at ultrasonic (10 MHz) frequencies, because short wavelengths are necessary to measure small tissue samples, and dispersion effects are expected to be small (see below).

Temperature and sound velocity

Temperature affects sound velocity in tissues. We were interested in estimating *in vivo* (37°C) sound velocity rather than room temperature (21°C) sound velocity so that future models can be representative of a living animal. A sample of
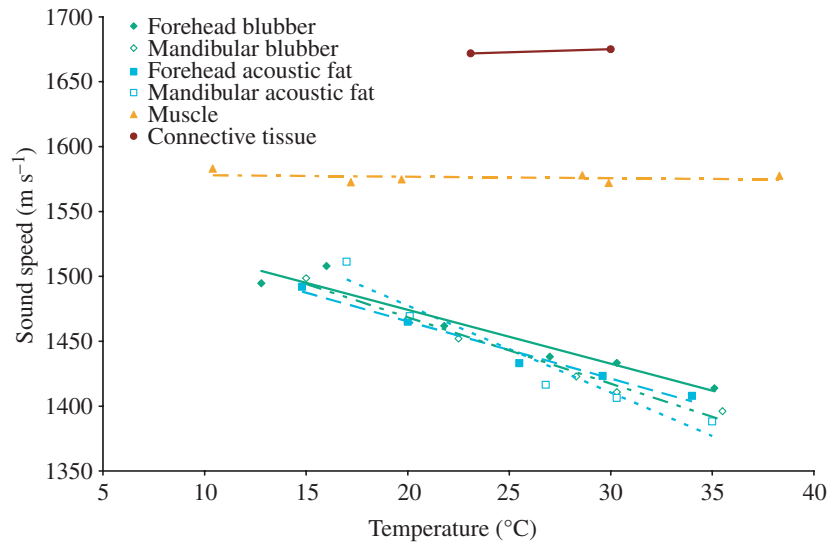

Fig. 4. Sound speed *versus* temperature from *Ziphius cavirostris* head tissues.

each type of tissue was placed in consecutive water baths at temperatures ranging from 10 to 37°C until the sample reached equilibrium, and its sound velocity was measured for each temperature.

Elasticity

Longitudinal compression tests of each sample were performed to measure the elastic modulus. Tissue materials exhibit a nonlinear relationship between stress and strain. We determined the elastic modulus as the tangent to the nonlinear stress–strain curve at different stresses. A Mini Bionix 858 (MTS Systems Corp., Eden Prairie, MN, USA) compressed each sample, while force and displacement data were recorded to a computer running TestStar (MTS Systems Corp.). The instrument was programmed to complete 10 low-stress cycles at 2 cycles s^{-1} with a 0.08 mm displacement, followed by one high-stress cycle at 0.5 cycles s^{-1} with a 2 mm displacement. Although these displacements may be large by acoustic standards, they enabled us to examine the nonlinearities in the tissues. The calipers that were used for the sound velocity measurements were also used to measure initial length of the tissue sample cube (i.e. initial distance between the compressing plates) and the area in contact with the plates. Each sample was placed in the instrument, and the hydraulic arm was engaged until the plates contacted the sample. If there was any initial force on the sample, it was recorded for use in

Table 2. *Results of sound speed–temperature analysis for various tissue types from the head of a* Ziphius cavirostris *neonate*

	Acoustic fat: forehead	Acoustic fat: mandible	Blubber: forehead	Blubber: mandible	Connective tissue	Muscle
Slope (*m*)	–4.4225	–7.113	–4.1655	–4.8081	0.4842	–0.116
r^2	0.979	0.946	0.932	0.953	–	0.080

Slopes and r^2 values of the best-fit line are presented.

later calculations, and the displacement gauge was zeroed prior to cycle loading the sample. We recorded force and displacement data at 100 samples s^{-1}. A customized MATLAB program provided stress *versus* strain plots for each sample. Hysteresis, a measure of the relative energy loss during elastic deformation, was calculated as the area between the loading curve and the recovery curve of the last low-stress cycle normalized by the total energy in the loading curve.

Density

Density was calculated using Archimedes' principle. We measured volume by immersing each sample in distilled water and weighing the displaced water. Water temperature was monitored to allow accurate calculations of density from water volume measurements. Wet mass was determined by direct measurement with a Mettler PM 460 Delta Range mass balance (Mettler-Toledo Inc., Columbus, OH, USA). Density was calculated by dividing mass by volume.

Statistical analysis

Sound velocity measurements were averaged across orientations, resulting in non-directional sound speed. We performed one-factor analyses of variance (ANOVAs) to compare values among tissue types for sound speed, sound attenuation, density, HU and hysteresis, followed by two-factor ANOVAs to compare values between locations (forehead or mandible) for blubber and acoustic fats (Zar, 1999). ANOVAs were followed up with a Scheffe *post-hoc* analysis (Zar, 1999). All ANOVAs were performed using SYSTAT (Systat Software Inc., Point Richmond, CA, USA). Student's *t*-tests were run to compare tissue type values with those of seawater at 15°C, 1 atm. (=101 kPa) and 35‰ salinity. Linear regressions and a principal components analysis (PCA) were run to investigate the relationships between the various measures. First, we averaged the values from the three orientations for sound velocity and elasticity. This enabled us to compare these measures to the density and HU measures that only had one value per sample. We performed linear regressions to determine the relationship between HUs and each of the other measures. We used PCA to determine the independence of the four physical property variables and to isolate the most important modes of variability in the data. PCA seeks linear combinations of variables that maximally explain the variance in the data (Jackson, 1991). The variance of a large data set is concentrated into a small number of physically interpretable patterns of variability – the principal components. Patterns among the physical property variables are illustrated by loadings on the principal components (Jackson, 1991).

Results

Temperature and sound speed

Sound speeds were plotted *versus* temperature for forehead blubber, forehead acoustic fats, mandibular blubber,
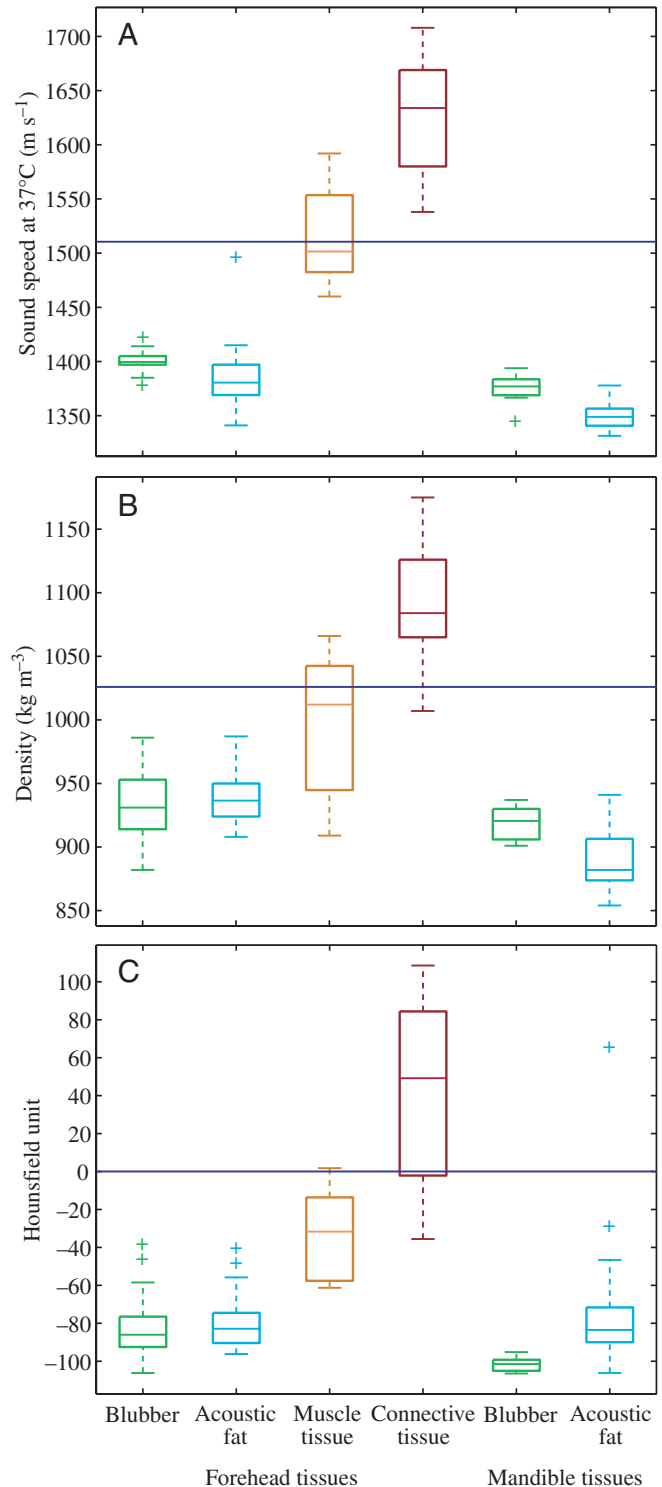

Fig. 5. Box and whisker plots of (A) sound speed corrected to 37°C, (B) mass density and (C) CT scan Hounsfield units for various tissue types in the forehead and mandible. The lines of the boxes represent the lower-quartile, median and upper-quartile values. The whiskers extending from each end of the box show the extent of the remaining data. Outliers are represented by + signs beyond the whiskers. The dark blue horizontal lines represent the sound speed (1507 m s^{-1}), density (1026 kg m^{-3}) and HU (0), respectively, of seawater at 15°C and 101 kPa.

Table 3. *Physical property measurements of* Ziphius cavirostris *forehead and mandibular tissues by tissue type*

	Forehead samples				Mandible samples	
	Blubber (*N*=36)	Acoustic fats (*N*=66)	Muscle (*N*=13)	Connective tissue (*N*=30)	Blubber (*N*=11)	Acoustic fats (*N*=44)
Sound speed at 37°C (m s^{-1})						
Mean	1401	1382	1517	1628	1376	1350
S.D.	7.8	23	46.8	48.7	13	10.6
Min.	1382	1341	1460	1538	1345	1331
Max.	1422	1409	1592	1708	1394	1378
Sound speed at 21°C (m s^{-1})						
Mean	1465	1450	1522	1620	1453	1460
S.D.	8.3	17.6	47.2	48.7	8.8	10.6
Min.	1446	1412	1461	1531	1441	1442
Max.	1489	1483	1594	1700	1468	1488
Density (kg m^{-3})						
Mean	935	937	993	1087	919	890
S.D.	25	17	58	41	13	23
Min.	882	908	909	1007	901	854
Max.	986	987	1066	1175	937	941
Hounsfield unit						
Mean	−84	−81	−33	45	−102	−78
S.D.	15	12	23	45	3	27
Min.	−106	−96	−61	−36	−106	−106
Max.	−46	−47	2	109	−95	−65
Hysteresis (%)						
Mean	28.4	32.5	–	53.5	21.7	29.4
S.D.	11.2	9.2	–	16.0	7.8	14.1
Min.	0.6	15.5	–	11.2	11.6	5.6
Max.	46.9	51.4	–	77.1	33.0	88.8

mandibular acoustic fats, muscle and connective tissue (Fig. 4). Sound speeds of all fatty tissues decreased with increasing temperature from 12°C to 35°C. Muscle sound speeds were nearly constant over the temperature range 10–37°C, as were connective tissue sound speeds over 22–30°C. Measured sound speeds were corrected to 37°C using the following equation:

$$V_{37} = V_o + (37 - T_o)\,m\,, \qquad (1)$$

where V_o is the measured sound speed, T_o is the measured temperature and m is the slope from the empirical data for each tissue type (Table 2). This correction enables comparison of sound speeds between samples, independent of temperature effects, as well as estimation of sound speed of various tissue types *in vivo*. Melon, connective tissue and muscle tissues are expected to be at 37°C *in vivo*. However, we expect a temperature gradient in blubber *in vivo* ranging from ambient seawater temperature at the skin boundary to body temperature at the internal boundary.

Sound speed

Sound speed values of *Ziphius cavirostris* head tissues ranged between 1331 and 1708 m s^{-1}. Sound speed values corrected to 37°C were significantly different between all tissue types (*P*≤0.001), with connective tissue exhibiting the highest sound speeds, followed by muscle, blubber and acoustic fats (Fig. 5; Table 3). Fatty tissues in the forehead region had significantly higher sound speeds than fatty tissues in the mandibular region (*P*≤0.001). The mean sound speed of seawater is 1507 m s^{-1} at 15°C, 101 kPa. and a salinity of 35‰ (Chen and Millero, 1977). Acoustic fats and blubber exhibit sound speeds significantly lower than those of seawater (*P*<0.05). Muscle tissues exhibit sound speeds that are not statistically different from seawater, while connective tissue sound speeds were significantly higher (*P*<0.05).

The organizational structure of the forehead tissues has a strong effect on sound speed. Across a lateral plane, sound speeds are lowest in the center of the forehead. However, in the posterior region, the low sound speed center shifts toward the right (Fig. 6). This change in sound speed is evident within the melon tissue as well as between tissue types. From anterior to posterior, the sound speeds are higher toward the rostrum where the melon fat grades into blubber. This increase is also evident toward the front of the forehead in the dorsal–ventral direction. In general, a low sound speed core is present that converges posteriorly, exhibiting spatial asymmetry and strong sound speed gradients. Anteriorly, the core is broader in size/shape, spatially symmetric and exhibits a low gradient toward the dorsal rostral side. Laterally, the gradient is sharp throughout the melon.
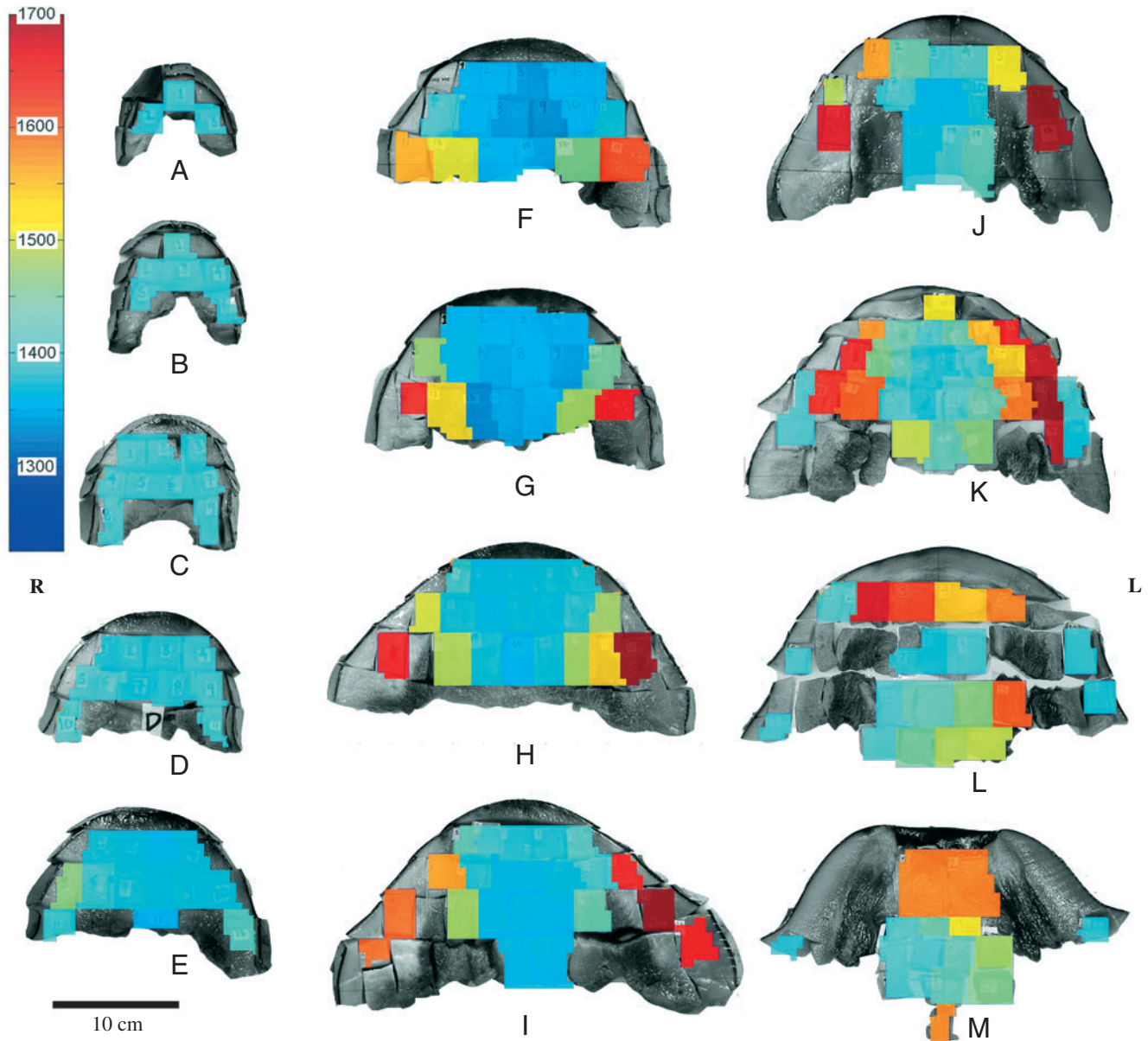
Fig. 6. Sound speed through 13 transverse slices (A–M) of *Ziphius cavirostris* melon. Slices N and O are not shown in this analysis since they encompass the nasal plugs. The figure shows the anterior face with dorsal side up. The animal's right (R) and left (L) sides are as shown in the figure. The color bar scale represents sound speed values (m s^{-1}).

Mass density

Cuvier's beaked whale tissue densities ranged from 854 to 1175 kg m^{-3}. All tissues exhibited significantly different density values from one another except blubber and acoustic fats. Connective tissues were densest, followed by muscle and then the fatty tissues (Table 3; Fig. 5). Acoustic fats in the mandibular region were significantly lower than forehead acoustic fats and all blubber tissues ($P \ll 0.001$). Seawater with a salinity of 35‰, at 15°C and 101 kPa has a mean density of 1026 kg m^{-3} (Pilson, 1998). Fatty tissues ($P < 0.05$) were significantly less dense than seawater, while muscle was not significantly different, and connective tissue was significantly denser than seawater ($P < 0.05$).

Hounsfield units

Hounsfield units in *Z. cavirostris* tissues ranged from −106 to 108 HU, with sampling standard deviations ranging from 1 to 30 HU. All tissues exhibited significantly different HU values from each other ($P \ll 0.001$), except for acoustic fats and blubber. Again, connective tissues exhibited the highest values, followed by muscle and then fatty tissues (Table 3; Fig. 5). In the mandible, blubber HU values were significantly lower than those of acoustic fats and forehead blubber ($P \ll 0.001$). Blubber, acoustic fats and muscle values were significantly lower than those for water, while connective tissue exhibited HU values significantly higher than those of water ($P < 0.05$).
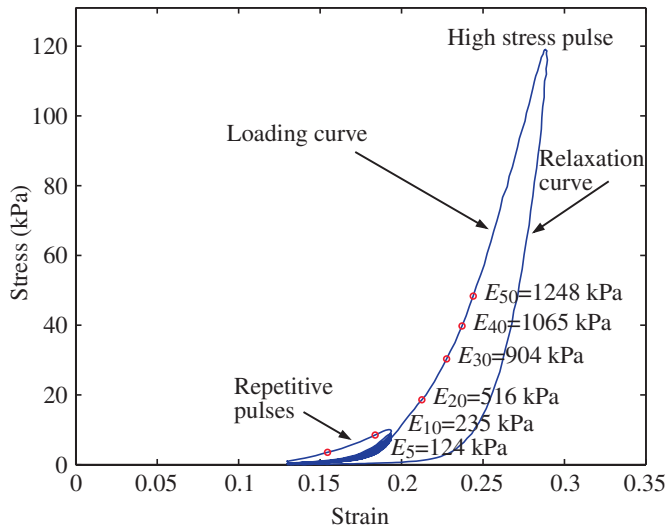
Fig. 7. Stress–strain curve for a sample of *Ziphius cavirostris* forehead blubber. The 10 low-stress pulses are visible at the low end of the curve, while the larger curve represents the single high-stress pulse.

Elasticity

Stress–strain curves were plotted for each of the samples from the data collected in the biomechanical compression tests (Fig. 7). Since the stress–strain curves were nonlinear, the elastic modulus (E) was evaluated at a variety of stresses to investigate how it changed with stress. These were averaged by tissue type and plotted against stress for the forehead and mandible tissues (Fig. 8). Muscle samples were discarded because myosin and actin connections, which are biologically important for retaining stiffness/structure, degrade with time after death (Schmidt-Nielsen, 1995).

Mean elastic modulus values for forehead and mandibular acoustic fat tissues ranged from 75 kPa to 934 kPa between stresses of 2.5 kPa and 50 kPa (Table 4). Blubber sample means from the forehead and mandibular regions ranged from 59 kPa to 1410 kPa at these stresses, and sample means for forehead connective tissue ranged from 124 to 1510 kPa. Across all stresses, acoustic fat samples had a lower elastic modulus for a given stress than did connective tissue and blubber. Blubber exhibits a nonlinear response in this strain range, becoming less compressible with increasing stress.

Percent hysteresis values in *Z. cavirostris* tissues ranged from 0.6 to 88.8%. Connective tissues exhibited significantly higher percent hysteresis than lipids ($P \ll 0.001$), while acoustic fats exhibited significantly higher percent hysteresis than blubber ($P=0.01$; Table 3). Lipids in the mandibular region had lower percent hysteresis than lipids in the forehead ($P=0.03$).

Correlations

Principal components analysis was run to search for combinations of tissue properties that vary together systematically. The results show that the first principal component explained 72% of the variance, while the second component explained 23%. Sound speed, density and HU were explained by the first principal component and are therefore dependant measures (Fig. 9). Elasticity was an independent measure and is explained by the second component. The samples are distributed in a nonrandom pattern, with similar tissues clumping together as shown in Fig. 10. The plot shows that the connective tissues, muscle and lipids separate out along the first component. On the other hand, melon and blubber can be distinguished by the second component.

Since sound speed, density and HU are measuring a similar characteristic, we looked for the linear correlations between the measured values and determined r^2 values for HU *versus* density and sound speed. Both measures showed a strong positive relationship to HU (Fig. 11). The relationship between HU and sound speed was stronger ($r^2=0.85$) than the one for HU and density ($r^2=0.76$).

Discussion

Sound speed

Several authors have discussed sound speed variations in the melons of marine Cetacea. Our measured sound speeds in the melon, ranging from 1412 to 1488 m s^{-1} at room temperature (Table 3), are higher than those reported for other cetaceans, where most room temperature values are around 1370 m s^{-1} (Apfel et al., 1985; Blomberg and Jensen, 1976; Blomberg and Lindholm, 1976; Litchfield et al., 1979; Norris and Harvey,
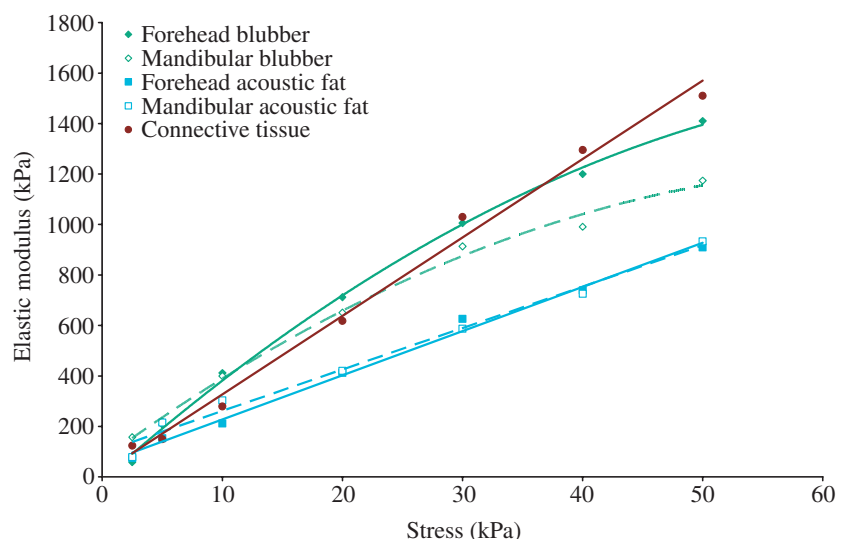

Fig. 8. Elastic modulus *versus* stress for tissues from a *Ziphius cavirostris* forehead and mandible. Blubber, acoustic fats and connective tissues are plotted for each location. Note that values have been averaged across three orientations (anterior–posterior, dorsal–ventral, lateral).

Table 4. *Mean elastic modulus (kPa) at selected stresses in the various tissue types of the forehead and mandible of a* Ziphius
cavirostris *neonate*

Stress (kPa)	Forehead tissues			Mandible tissues	
	Blubber	Acoustic fat	Connective tissue	Blubber	Acoustic fat
2.5	59	75	124	158	78
5	208	153	149	220	215
10	411	212	279	400	303
20	712	412	618	650	420
30	1006	626	1030	913	587
40	1200	739	1295	991	726
50	1410	910	1510	1174	934

1974). The study by Norris and Harvey (1974) had the most comparable values, with sound speeds ranging from 1273 to 1481 m s^{-1}. These differences may be due to technique: most studies extracted the oils from the tissues to perform sound speed tests, while our study and that of Norris and Harvey (1974) used the actual tissues. Another important difference of our study is that the subject was a neonate. Koopman et al. (2003a) and Lok and Folkersma (1979) have shown ontogenetic changes in beaked whale melon lipid composition, which may be reflected in changes of sound speed and transmission properties. However, sound speed differences may also reflect real differences between beaked whales and other cetaceans, as evidenced by differences in melon lipid chemistry (Litchfield et al., 1976).

Previous studies of sound speed in the odontocete forehead have reported a low sound speed inner core within the melon, consistent with the results of our study (Flewellen and Morris, 1987; Litchfield et al., 1979; Norris and Harvey, 1974). The presence of a low sound speed core supports the hypothesis that the beaked whale melon helps to produce a directional sound beam. The structure of the forehead, involving different tissues components, may give rise to stages of directional sound beam formation. For example, air spaces, dense

connective tissue layers and bony regions can act as acoustically reflective surfaces that function to direct sound anteriorly. Another stage of beam formation results from the chemical topography in the melon, which tends to focus the beam along the low sound speed core.

The increase in sound speed between melon and blubber may be important in impedance matching of the sound waves to the water to maximize the acoustic energy transfer out of the forehead. Impedance matching occurs when the acoustic impedances (the product of density and sound speed) of two adjacent materials are similar, resulting in greater transmission of acoustic energy at the boundary between the two materials. Another factor that influences sound speed, and thereby impedance matching, is the change in temperature from the interior to exterior boundaries of the blubber. At the interior, sound speed averages 1401 m s^{-1} for 37°C blubber, which increases to 1492 m s^{-1} at the exterior blubber boundary in 15°C water (see Table 2), which has a sound speed of 1507 m s^{-1}. These results support acoustic impedance matching between the melon, blubber and seawater as a proposed function for the
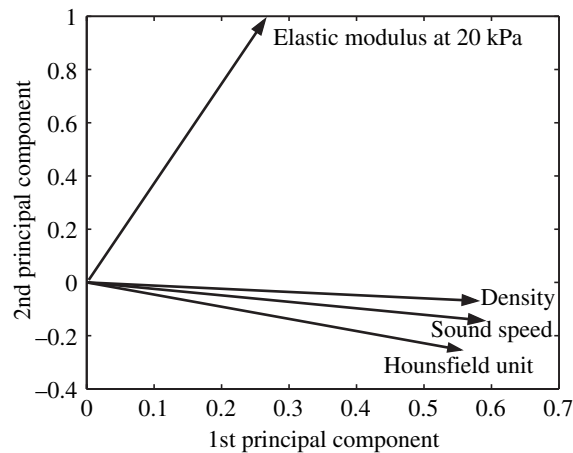

Fig. 9. Results of a principal components analysis showing the loadings of each variable for the first two principal components. Density, Hounsfield unit and sound speed are all described primarily by the 1st principal component, while elastic modulus is described by the 2nd principal component.
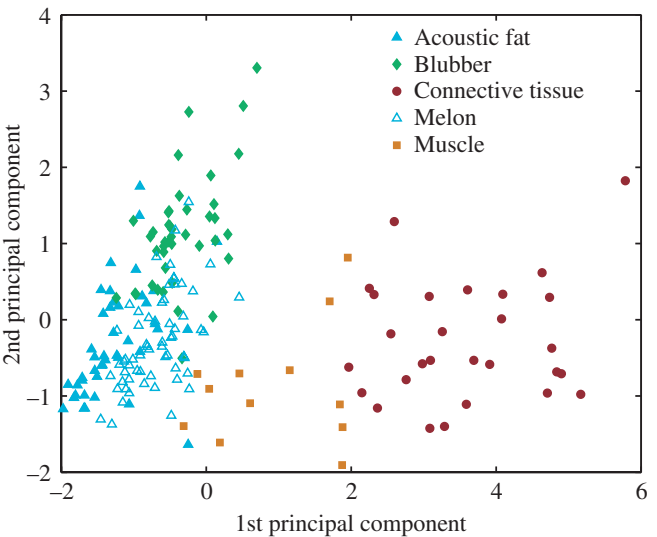

Fig. 10. Scatter plot of 1st and 2nd principal component loadings for each *Ziphius cavirostris* tissue sample. Lipids, muscle and connective tissue can be distinguished from each other by the first component, while acoustic fats are distinguished from blubber by the second component.

Cuvier's beaked whale melon, as proposed for the bottlenose dolphin melon (Norris and Harvey, 1974). Sound speed in the fats in the mandibular channel also exhibit low sound speeds compared with surrounding tissues. Again, the change in sound speed from seawater to blubber to acoustic fat is probably important in impedance matching for sound reception and the channeling of sound from seawater to the ear complexes.

Sound speed values for cetacean blubber, muscle and connective tissue are not present in the literature; however, values for terrestrial mammal fats, muscle and collagen fibers (a main component of connective tissue) are available. Our *Z. cavirostris* sound speed values for blubber at 21°C (ranging from 1453 to 1489 m s^{-1}) are consistent with those reported for terrestrial mammals (1412–1489 m s^{-1} for human, cow, dog and pig fat; reviewed by Duck, 1990). The sound speed values for most *Z. cavirostris* muscle samples at 21°C (ranging from 1461 to 1594 m s^{-1}) are also similar to those reported for terrestrial mammals (1542–1631 m s^{-1} for human, cow, dog, pig and rabbit muscle; reviewed by Duck, 1990; O'Brien, 1977), but values for muscles found in the forehead region extend lower. Forehead region muscles appear to have increased lipid content compared with muscle tissues found throughout the body (Soldevilla et al, 2004), which leads to a decrease in sound speed (Duck, 1990). Very little has been published on connective tissue sound speed; however, one study reports collagen sound speed at 1570 m s^{-1} (reviewed in Duck, 1990; Lees and Rollins, 1972). *Ziphius cavirostris* connective tissue values exhibited a large range (1538–1708 m s^{-1} at 21°C), which is probably due to the high variability in connective tissues that exhibit complex collagen structures. Collagen content in tissues affects sound speed significantly (O'Brien, 1977) such that the range of sound speed values may be associated with relative proportions of water and collagen in the samples.

The results of our temperature–sound speed experiments are similar to those reported by others. Our study of fats shows a linear decrease in sound speed with increasing temperature of ~4 m s^{-1} deg.$^{-1}$, while muscle and connective tissue had a nearly constant slope. Duck (1990) reports that sound speed in fats decreases linearly with increasing temperature (at ~10 m s^{-1} deg.$^{-1}$) until ~35°C, where it exhibits nonlinear behavior and decreases at a lower rate. Studies have investigated sound speed changes with temperature in forehead acoustic fats in marine mammals. Lipids extracted from melon tissues decrease with increasing temperature, in the order of 1–13 m s^{-1} deg.$^{-1}$ (Blomberg and Jensen, 1976; Goold et al.,
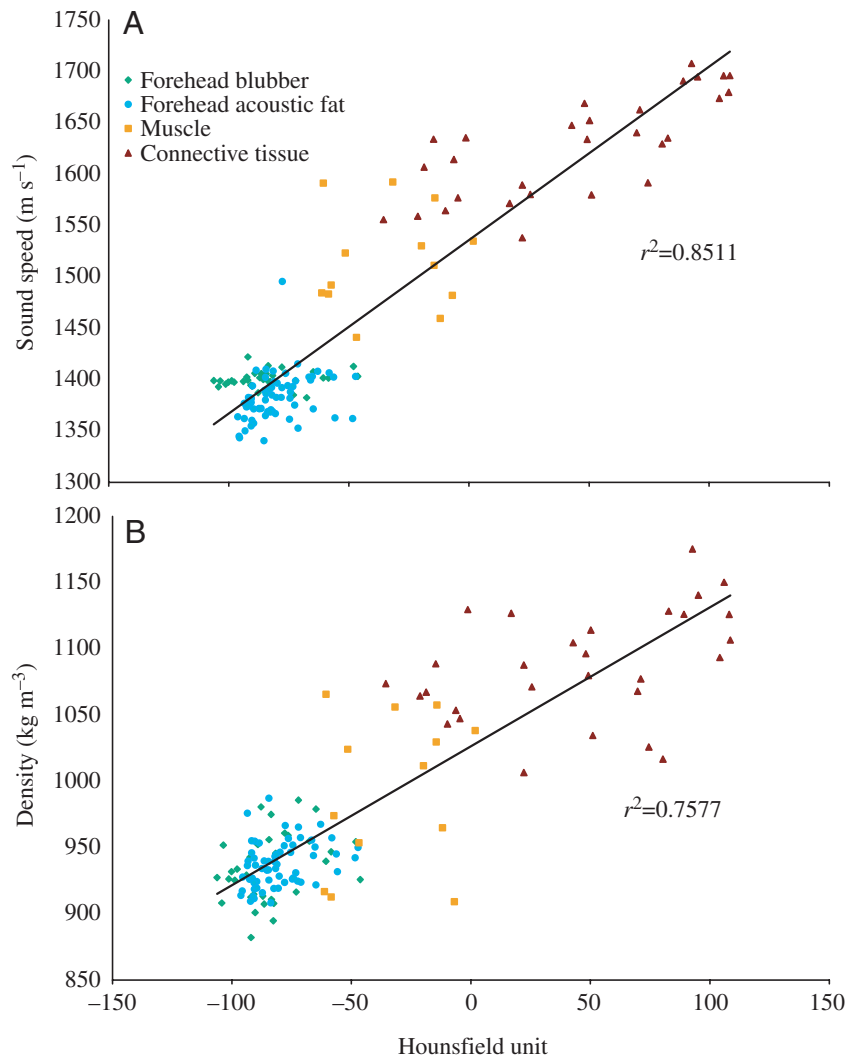

Fig. 11. Regression analysis of Hounsfield units *versus* (A) sound speed and (B) density for *Ziphius cavirostris* forehead tissues. Best-fit lines are represented by the following equations: sound speed=1.6889HU+1535.9; density=0.001HU+1.0265.

1996; Goold and Clarke, 2000; Litchfield et al., 1979). These studies (except Litchfield et al., 1979) have shown a nonlinear effect due to the phase change of the oils near body temperature. This is an important finding since beaked whale melon/acoustic fats have a different lipid composition, particularly in neonates, yet the lipids exhibit the same pattern of properties. We were not able to investigate nonlinear changes around body temperature since the tissues in our samples exhibited a phase change. It would be important to study this effect in beaked whale tissues in the future to better understand how the melon functions for sound conduction.

Mass density

Mass densities of the *Z. cavirostris* tissue types are similar to those found in other mammals. Fatty tissues in this study ranged from 854 to 987 kg m^{-3}, averaging 922 kg m^{-3}. Duck (1990) reports mean human fat densities ranging from 917 to 939 kg m^{-3} (human breast fat) and 990 to 1060 kg m^{-3} (human

breast including all tissues). The lower values that we found therefore correspond to pure fatty tissues, while the higher values include more structural tissues such as collagen in blubber. Our *Z. cavirostris* muscle values (ranging from 909 to 1066 kg m^{-3}) are similar to those reported for terrestrial mammals (ranging from 1038 to 1056 kg m^{-3}; Duck, 1990) but extend lower, suggesting the presence of lipids in forehead muscle tissues.

Hounsfield unit

Ziphius cavirostris fats, including acoustic fats and blubber, had CT scan HU values ranging from –106 to –46. Robb (1998) found that mammalian fat values typically lie between –100 and –70. Most of our samples lie within this range; however, some blubber and melon fat samples from the forehead exhibited higher HU values than Robb found. This may be due to human error in matching the locations of the samples in the CT scan to their geometric space from dissection. It may also indicate that changes are due to the unique lipid chemistry of odontocete blubber and acoustic fats compared with common mammal fats or the presence of collagen in the blubber. This is a topic that merits further investigation.

Muscle HU values typically fall between 25 and 60 HU (Robb, 1998). Our values ranged from –61 to 2. These are lower than those reported by Robb, which may be caused by lipid content in the forehead muscle, which would decrease the HU value. Goodpaster et al. (2000) found that human skeletal muscle containing high lipid concentrations exhibited lower HU values than muscle that contained low lipid concentrations. The differences in our values might also be due to the amount of *postmortem* time and consequent decomposition in muscle tissues, perhaps the most susceptible to these changes.

Elasticity

Elastic modulus values for *Z. cavirostris* tissues range between 0.1 and 1.5 MPa at stresses from 2.5 to 50 kPa. Connective tissue and blubber exhibit the full range of values above, with elastic modulus increasing with increasing stress. Melon, on the other hand, exhibits lower values, with a high of 0.93 MPa at 50 kPa. The higher values for blubber and connective tissue suggest that these tissues have greater structure than melon, which is reasonable since connective tissue and blubber are held together by collagen fibers. O'Brien (1977) notes that the elastic properties of soft tissue are determined primarily by the content of collagen and other structural proteins. Elastic moduli for tissues vary nonlinearly with applied stress, making comparisons with previously published values difficult as these measurements may have been carried out on different portions of the stress–strain curve. Percent hysteresis values for *Z. cavirostris* fall in the typical range for mammalian tissues. Collagen exhibits low values (7%), while materials like silk exhibit high values (65%), with the majority of tissues falling around 20% (Vogel, 1988).

Correlations

The results of the PCA show that connective tissue, muscle and lipids separate distinctly along the first principal component (Fig. 10), which represents sound speed, density and HU (Fig. 9). This separation shows that sound speed, density or HU can each be used to determine the type of tissue in a Cuvier's beaked whale, since each tissue type's physical properties are distinct. The high explanatory power of the first principal component illustrates that sound speed, density and HU are measuring similar characteristics. This supports the notion that HUs can be used to model density and sound speed parameters needed for acoustic modeling, which is beneficial to modeling efforts, since HUs can be collected throughout a whole specimen non-destructively. Hounsfield units cannot be used to predict elastic modulus values. Elasticity, primarily represented by the second principal component, is the only measure that distinguishes between acoustic fats and blubber (Fig. 10). Elasticity is important for understanding the behavior of these tissues under high stress conditions.

The linear correlations between HUs and sound speed and density were high (0.85 and 0.76, respectively). The linear relationships we found for these measures provide a model to determine the sound speed and density when only the HUs from CT scanning are available (Fig. 11). Some of the noise in the data may be due to human error in correlating the samples to their location in the CT scans. Future studies should work to improve this method.

Limitations

Our analysis of the physical properties of Cuvier's beaked whale tissues provides improvements on past research and insight into sound generation, reception and acoustic trauma modeling. However, the results do have some limitations. (1) Sound speed measurements were made at 10 MHz, while the frequencies of interest range from 1 to 200 kHz. Sound speed dispersion for biological soft tissues and marine mammal oils ranges from 1 to 10 m s^{-1} between 1 and 10 MHz (Cartensen and Schwan, 1959; Kremkau et al., 1981; Kuo and Weng, 1975; O'Donnell et al., 1981). While our values may be a few m s^{-1} too high, this is within the error of our measurements. (2) The specimen we studied was a neonate. H. N. Koopman, S. M. Budge, D. R. Ketten and S. J. Iverson (personal communcation) have described ontogenetic changes in the chemical makeup of acoustic fats in beaked whales that may affect physical properties of tissues. This is an important distinction for sound generation and reception modeling. However, *Ziphius cavirostris* specimens are not readily available. The present study is the first to present any physical property data from a Cuvier's beaked whale. (3) Temperature–sound speed measurements were not carried out at 37°C, our estimated *in vivo* temperature. Sound speed in lipids exhibits nonlinear changes around body temperature, suggesting that our calculated sound speeds may be a few m s^{-1} too low. It would be important to study this effect in beaked whale tissues in the future to better understand how the melon functions for sound conduction. (4) Histological analysis of tissue categories was beyond the scope of our study. Variations in tissue content of each sample could have led to the variation we see in our results. (5) Measurements

were made on thawed, *postmortem* tissues. Changes in tissue physical properties may arise after death, and with freezing. No significant changes were found for melon fat, blubber and connective tissue CT scan HU values in live, recently deceased and frozen bottlenose dolphin specimens (M. F. McKenna, personal communication). No significant differences have been found for sound speeds in bottlenose dolphin tissues as a function of time after death and freezing (M. F. McKenna, personal communication). The same results were found for sound speeds in fresh and frozen mammalian liver (Van der Steen et al, 1991), myocardial tissues (Dent et al., 2000) and human breast tissue (Foster et al., 1984). Elastic properties of thawed non-contractile tissues, including human intervertebral discs and rabbit ligaments, are not significantly different from fresh samples (Smeathers and Joanes, 1988; Woo et al., 1986). Fitzgerald (1975) and Fitzgerald and Fitzgerald (1995) suggest there is a life-to-death transition in visco-elastic compliance for beef fat, porcine intervertebral disc and whale blubber around 5–11 h *postmortem*. Significant changes in the elastic properties of contractile muscle tissues result from the *postmortem* and freezing process (Leitschuh et al., 1996; Gottsauner-Wolf et al., 1995; Van Ee et al., 2000). In summary, sound speed and CT scan HU values are not significantly affected by *postmortem* and freezing processes. Elastic properties of non-contractile tissues may exhibit *postmortem* differences but are not affected by freezing, and elastic properties of contractile tissues are significantly affected by *postmortem* and freezing effects. For this reason, we have discarded muscle from our analysis of elastic properties.

Conclusion

This study provides high topographical resolution data on sound speed, mass density, CT scan Hounsfield units and elasticity for *Z. cavirostris* tissues. This has been the first attempt at gathering this breadth of physical property data from beaked whale tissues. We have examined the similarities and differences that exist between these properties from Cuvier's beaked whale tissues, which have unique structural and chemical characteristics, and those found in other marine and terrestrial mammals. Evidence for a relationship between CT scan HUs and sound speed and mass density is presented. This may allow future studies to relate CT scan values from *Z. cavirostris* to these physical properties without extracting tissue samples. While there are limitations to our methods and results, the data we present show promise for use in acoustic-structural models of a beaked whale that may provide insight into sound emission and reception paths and into possible mechanisms for *Z. cavirostris*' sensitivity to sound.

References

Apfel, R. E., Young, R. E., Varanasi, U., Maloney, J. R. and Malins, D. C. (1985). Sound velocity in lipids, oils, waxes, and their mixtures using an acoustic levitation technique. *J. Acoust. Soc. Am.* **78**, 868-870.
Aroyan, J. L. (2001). Three-dimensional modeling of hearing in *Delphinus delphis*. *J. Acoust. Soc. Am.* **110**, 3305-3318.
Aroyan, J. L., Cranford, T. W., Kent, J. and Norris, K. S. (1992). Computer modeling of acoustic beam formation in *Delphinus delphis*. *J. Acoust. Soc. Am.* **92**, 2539–2545.
Au, W. W. L. (1993). *The Sonar of Dolphins.* New York: Springer-Verlag.
Baird, R. W., McSweeney, D. J., Ligon, A. D. and Webster, D. L. (2004). *Tagging Feasibility and Diving of Cuvier's Beaked Whales (*Ziphius cavirostris*) and Blainville's Beaked Whales (*Mesoplodon densirostris*) in Hawaii. Report Prepared Under Order No. AB133F-03-SE-0986 to the Hawaii Wildlife Fund, Volcano, HI.* La Jolla, CA, USA: Southwest Fisheries Science Center, National Marine Fisheries Service.
Barlow, J., Forney, K., VonSaunder, A. and Urban-R, J. (1997). *A Report of Cetacean Acoustic Detection and Dive Interval Studies (CADDIS) Conducted in the Southern Gulf of California, 1995. NOAA Technical Memorandum.* NOAA-TM-NMFS-SWFSC-250. La Jolla, CA, USA: Southwest Fisheries Science Center, National Marine Fisheries Service.
Blanco, C. and Raga, J. A. (2000). Cephalopod prey of two *Ziphius cavirostris* (Cetacea) stranded on the western Mediterranean coast. *J. Mar. Biol. Assoc. UK* **80**, 381-382.
Blomberg, J. and Jensen, B. N. (1976). Ultrasonic studies on the head oil of the North Atlantic pilot whale (*Globicephala melaena melaena*). *J. Acoust. Soc. Am.* **60**, 755-759.
Blomberg, J. and Lindholm, L. E. (1976). Variations in lipid composition and sound velocity in melon from the North Atlantic pilot whale, *Globicephala melaena melaena*. *Lipids* **11**, 153-156.
Boutiba, Z. (1994). A review of our knowledge on the presence of cetaceans off the Algerian coasts. *Mammalia* **58**, 613-622.
Brill, R. L., Sevenich, M. L., Sullivan, T. J., Sustman, J. D. and Witt, R. E. (1988). Behavioral evidence for hearing through the lower jaw by an echolocating dolphin Tursiops truncatus. *Mar. Mammal Sci.* **4**, 223-230.
Cartnesen, E. L. and Schwan, H. P. (1959). Acoustic properties of hemoglobin solutions. *J. Acoust. Soc. Am.* **31**, 305-311.
Chen, C. T. and Millero, F. J. (1977). Speed of sound in seawater at high pressures. *J. Acoust. Soc. Am.* **62**, 1129-1135.
Cranford, T. W., Amundin, M. and Norris, K. S. (1996). Functional morphology and homology in the odontocete nasal complex: Implications for sound generation. *J. Morphol.* **228**, 223-285.
Crum, L. A. and Mao, Y. (1996). Acoustically enhanced bubble growth at low frequencies and its implications for human diver and marine mammal safety. *J. Acoust. Soc. Am.* **99**, 2898-2907.
D'Amico, A., Bergamasco, A., Zanasca, P., Carniel, S., Nacini, E., Portunato, N., Teloni, V., Mori, C. and Barbanti, R. (2003). Qualitative correlation of marine mammals with physical and biological parameters in the Ligurian Sea. *IEEE J. Oceanic Eng.* **28**, 29-43.
Dent, C. L., Scott, M. J., Wickline, S. A. and Hall, C. S. (2000). High-frequency ultrasound for quantitative characterization of myocardial edema. *Ultrasound Med. Biol.* **26**, 375-384.
Duck, F. A. (1990). *Physical Properties of Tissue: A Comprehensive Reference Book.* San Diego: Academic Press.
Evans, D. L. and England, G. R. (2001). *Joint Interim Report. Bahamas Marine Mammal Stranding Event of 14-16 March 2000.* Washington DC, USA: US Department of Commerce and US Navy.
Fernández, A. (2004). Pathological findings in stranded beaked whales during the naval military manoeuvers near the Canary Islands. In *Proceedings of the Workshop on Active Sonar and Cetaceans.* European Cetacean Society newsletter **42**, second edn. (ed. P. G. H. Evans and L. A. Miller), pp. 37-40.

Fiscus, C. H. (1997). Cephalopod beaks in a Cuvier's beaked whale (*Ziphius cavirostris*) from Amchitka Island, Alaska. *Mar. Mammal Sci.* **13**, 481-486.

Finneran, J. J. (2003). Whole-lung resonance in a bottlenose dolphin (*Tursiops truncatus*) and white whales (*Delphinapterus leucas*). *J. Acoust. Soc. Am.* **114**, 529-535.

Fitzgerald, E. R. (1975). Dynamic mechanical measurements during the life to death transition in animal tissues. *Biorheology* **12**, 397-408.

Fitzgerald, E. R. and Fitzgerald, J. W. (1995). Blubber and compliant coatings for drag reduction in water. I. Viscoelastic properties of blubber and compliant coating materials. *Mater. Sci. Eng.* **C2**, 209-214.

Flewellen, C. G. and Morris, R. J. (1978). Sound velocity measurements on samples from the spermaceti organ of the sperm whale (*Physeter catadon*). *Deep-Sea Res.* **25**, 269-277.

Forney, K. A., Barlow, J. and Carretta, J. V. (1995). The abundance of cetaceans in California waters II. Aerial surveys in winter and spring of 1991 and 1992. *Fish. B.-NOAA* **93**, 15-26.

Foster, F. S., Strban, M. and Austin, G. (1984). The ultrasound macroscope: initial studies of breast tissue. *Ultrasonic Imaging* **6**, 243-261.

Frantzis, A. (1998). Does acoustic testing strand whales? *Nature* **392**, 29.

Goodpaster, B. H., Kelley, D. E., Thaete, F. L., He, J. and Ross, R. (2000). Skeletal muscle attenuation determined by computed tomography is associated with skeletal muscle lipid content. *J. Appl. Physio.* **89**, 104-110.

Goold, J. C., Bennell, J. D. and Jones, S. E. (1996). Sound velocity measurements in spermaceti oil under the combined influences of temperature and pressure. *Deep-Sea Res.* **43**, 961-969.

Goold, J. C. and Clarke, M. R. (2000). Sound velocity in the head of the dwarf sperm whale, *Kogia sima*, with anatomical and functional discussion. *J. Mar. Biol. Assoc. UK* **80**, 535-542.

Gottsauner-Wolf, F., Grabowski, J. J., Chao, E. Y. S. and An, K. N. (1995). Effects of freeze/thaw conditioning on the tensile properties and failure mode of bone-muscle-bone units: a biomechanical and histological study in dogs. *J. Orthop. Res.* **13**, 90-95.

Heyning, J. E. (1989a). Comparative facial anatomy of beaked whales (Ziphiidae) and a systematic revision among the families of extant Odontoceti. *Contrib. Sci.* **405**, 1-64N.

Heyning, J. E. (1989b). Cuvier's beaked whale Ziphius cavirostris G. Cuvier 1823. In *Handbook of Marine Mammals. Volume 4, River Dolphins and the Larger Toothed Whales* (ed. S. H. Ridgway and Sir R. Harrison), pp. 289-308. New York: Academic Press.

Heyning, J. E. and Mead, J. G. (1990). Evolution of the Nasal Anatomy of Cetaceans. In *Sensory Abilities of Cetaceans* (ed. J. Thomas and R. Kastelein), pp. 67-79. New York: Plenum Press.

Houser, D. S., Howard, R. and Ridgway, S. (2001). Can diving-induced tissue nitrogen supersaturation increase the chance of acoustically driven bubble growth in marine mammals? *J. Theoret. Biol.* **213**, 183-195.

Houston, J. (1991). Status of Cuvier beaked-whale, *Ziphius cavirostris*, in Canada. *Can. Field Nat.* **105**, 215-218.

Jackson, J. E. (1991). *A User's Guide to Principal Components*. New York: John Wiley & Sons.

Jepson, P. D., Arbelo, M., Deaville, R., Patterson, I. A. P., Castro, P., Baker, J. R., Degollada, E., Ross, H. M., Herraez, P., Pocknell, A. M. et al. (2003). Gas-bubble lesions in stranded cetaceans–Was sonar responsible for a spate of whale deaths after an Atlantic military exercise? *Nature* **425**, 575-576.

Johnson, M., Madsen, P. T., Zimmer, W. M. X., Aguilar de Soto, N. and Tyack, P. L. (2004). Beaked whales echolocate on prey. *Proc. R. Soc. London Ser. B* **Suppl.** 04BL0042.S1-S4.

Koopman, H. N., Iverson, S. J. and Read, A. J. (2003). High concentrations of isovaleric acid in the fats of odontocetes: variation and patterns of accumulation in blubber vs. stability in the melon. *J. Comp. Physiol. B* **173**, 247-261.

Kremkau, F. W., Barnes, R. W. and McGraw, C. P. (1981). Ultrasonic attenuation and propagation speed in normal human brain. *J. Acoust. Soc. Am.* **70**, 29-38.

Kuo, H. L. and Weng, J. S. (1975). Temperature and frequency dependence of ultrasonic velocity and absorption in sperm and seal oils. *J. Am. Oil Chem. Soc.* **52**, 16-169.

Lawrence, B. and Schevill, W. E. (1956). The functional anatomy of the Delphinid nose. *Bull. Mus. Comp. Zool.* **114**, 103-151.

Lees, S. and Rollins, F. R. (1972). Anisotropy in hard dental tissues. *J. Biomech.* **5**, 557-566.

Leitschuh, P. H., Doherty, T. J., Taylor, D. C., Brooks, D. E. and Ryan, J. B. (1996). Effects of postmortem freezing on tensile failure properties of rabbit extensor digitorum longus muscle tendon complex. *J. Orthopaed. Res.* **14**, 830-833.

Lillie, R. D. (1977). *Cohn's Biological Stains: A Handbook on the Nature and Uses of the Dyes Employed in the Biological Laboratory.* 9th edn. 692pp. Baltimore, MD, USA: Williams and Wilkins Co.

Litchfield, C., Karol, R. and Greenberg, A. J. (1973). Compositional topography of melon lipids in the Altantic Bottlenosed dolphin *Tursiops truncatus*: Implications for echo-location. *Mar. Biol.* **23**, 165-169.

Litchfield, C., Greenberg, A. J. and Mead, J. G. (1976). The distinctive character of Ziphiidae head and blubber fats. *Cetology* **23**, 1-10.

Litchfield, C., Karol, R., Mullen, M. E., Dilger, J. P. and Luthi, B. (1979). Physical factors influencing refraction of the echolocative sound beam in delphinid cetaceans. *Mar. Biol.* **52**, 285-290.

Lok, C. M. and Folkersma, B. (1979). Composition of wax esters and triacylglycerols in the melon and blubber fats of a young Sowerby's whale *Mesoplodon bidens*. *Lipids* **14**, 872-875.

MacLeod, C. D., Santos, M. B. and Pierce, G. J. (2003). Review of data on diets of beaked whales: evidence of niche separation and geographic segregation. *J. Mar. Biol. Assoc. UK* **83**, 651-665**.**

Marini, L., Consiglio, C., Angradi, A. M., Catalano, B., Sanna, A., Valentini, T., Finoia, M. G. and Villetti, G. (1996). Distribution, abundance and seasonality of cetaceans sighted during scheduled ferry crossings in the central Tyrrhenian Sea: 1989-1992. *Ital. J. Zool.* **63**, 381-388.

Mead, J. (1975). Anatomy of the External Nasal Passages and Facial Complex in the Delphinidae (Mammalia: Cetacea). *Smithsonian Contrib. Zool.* **207**, 1-72.

Norris, K. S. (1964). Some problems of echolocation in cetaceans. In *Marine Bioacoustics* (ed. W. Tavolga), pp. 317–336. New York: Pergamom Press.

Norris, K. S. and Harvey, G. W. (1974). Sound transmission in the porpoise head. *J. Acoust. Soc. Am.* **56**, 659-664.

O'Brien, W. D. (1977). The relationship between collagen and ultrasonic attenuation and velocity in tissue. *Ultrasonics Int.* **77**, 194-205.

O'Donnell, M., Jaynes, E. T. and Miller, J. G. (1981). Kramers-Kronig relationship between ultrasonic attenuation and phase velocity. *J. Acoust. Soc. Am.* **63**, 1935-1937.

Pilson, M. E. Q. (1998). *An Introduction to the Chemistry of the Sea*. New Jersey: Prentice Hall.

Robb, R. A. (1998). *Three-dimensional Biomedical Imaging: Principles and Practice.* New York: John Wiley & Sons.

Santos, M. B., Pierce, G. J., Herman, J., Lopez, A., Guerra, A., Mente, E. and Clarke, M. R. (2001). Feeding ecology of Cuvier's beaked whale (*Ziphius cavirostris*): a review with new information on the diet of this species. *J. Mar. Biol. Assoc. UK* **81**, 687-694.

Schmidt-Nielsen, K. (1995). *Animal Physiology: Adaptation and Environment*, 4th edn. New York: Cambridge University Press.

Simmonds, M. P. and Lopez-Jurado, L. F. (1991). Whales and the military. *Nature* **351**, 448-448.

Smeathers, J. E. and Joanes, D. N. (1988). Dynamic compressive properties of human lumbar intervertebral joints: A comparison between fresh and thawed specimens. *J. Biomech.* **21**, 425-433.

Soldevilla, M. S., McKenna, M. F., Wiggins, S. M., Shadwick, R. E., Cranford, T. W. and Hildebrand, J. A. (2004). *Cuvier's Beaked Whale (*Ziphius cavirostris*) Tissue Physical Properties: Measurements of Sound Speed/Attenuation, Density, CT numbers, Elasticity, and Temperature Influences. Marine Physical Laboratory Technical Memorandum* no. 480. La Jolla, CA, USA: Scripps Institution of Oceanography.

Van der Steen, A. F. W., Cuypers, M. H. M., Thijssen, J. M. and de Wilde, P. C. M. (1991). Influence of histochemical preparation on acoustic parameters of liver tissue: A 5-MHz study. *Ultrasound Med. Bio.* **17**, 879-891.

Van Ee, C. A., Chasse, A. L. and Meyers, B. S. (2000). Quantifying skeletal muscle properties in cadaveric test specimens: Effects of mechanical loading, postmortem time, and freezer storage. *J. Biomech. Eng-T. Asme* **122**, 9-14.

Varanasi, U., Markey, D. and Malins, D. C. (1982). Role of isovaleroyl lipids in channeling of sound in the porpoise melon. *Chem. Phys. Lipids* **31**, 237-244.

Waring, G. T., Hamazaki, T., Sheehan, D., Wood, G. and Baker, S. (2001). Characterization of beaked whale (Ziphiidae) and sperm whale (*Physeter macrocephalus*) summer habitat in shelf-edge and deeper waters off the northeast US. *Mar. Mammal Sci.* **17**, 703-717.

Woo, S. L. Y., Orlando, C. A., Camp, J. F. and Akeson, W. H. (1986). Effects of postmortem storage by freezing on ligament tensile behavior. *J. Biomech.* **19**, 399-404.

Zar, J. H. (1999). *Biostatistical analysis*. 4th edn. Upper Saddle River: Prentice Hall.